Validity of the effective-medium approximation of photonic crystals

Wojciech Śmigaj* and Boris Gralak†
Institut Fresnel, UMR CNRS 6133, Faculté des Sciences et Techniques, Université Paul Cezanne Aix-Marseille III, 13397 Marseille Cedex 20, France

(Received 5 February 2008; revised manuscript received 28 May 2008; published 30 June 2008)

A definition of the effective permittivity and permeability is proposed for two-dimensional photonic crystals. Expression for these effective parameters is deduced from the combination of the dispersion law with the formula for the reflection coefficient of a semi-infinite photonic crystal in the *single-mode approximation*. From these expressions, it is shown that the effective permittivity and permeability take purely real values when the truncation plane of the photonic crystal contains an inversion center of the infinite crystal. In addition, these effective parameters are demonstrated to be continuous and bounded when the crystal mode turns from propagating to evanescent only if the eigenmode fields fulfill specific symmetry conditions. Finally, the validity of the single-mode approximation and the effective-medium model of photonic crystals is investigated. In particular, arguments suggesting that this model fails for bands exhibiting negative refraction are presented.

DOI: 10.1103/PhysRevB.77.235445 PACS number(s): 42.70.Qs, 78.20.Ci, 42.25.Gy

I. INTRODUCTION

A crucial feature of photonic crystals (PCs) is the richness of their dispersion relation.[1] As opposed to homogeneous media, whose equifrequency surfaces are always ellipsoidal—and, consequently, convex—the shape of PC equifrequency surfaces can be very complex: they can contain sharp corners or edges separating flat or even concave areas. This gives rise to unusual phenomena,[2] in particular, the self-collimation of light[3] and the superprism effect.[4] However, at specific frequencies, the equifrequency surfaces of PCs can attain ellipsoidal shape too. In consequence, the question arises if the electromagnetic behavior of the crystals can then be successfully described in the effective-medium approximation, where the crystal in question is replaced with a homogeneous material with definite values of permittivity ϵ and permeability μ or, equivalently, refractive index $n=\sqrt{\epsilon\mu}$ and impedance $\eta=\sqrt{\mu/\epsilon}$. This procedure is especially tempting in the analysis of photonic devices employing the negative-refraction effect,[5] where the behavior of the corresponding system made of ideally homogeneous materials is usually known in advance—a famous example being the "perfect lens."[6]

Numerous papers dealing with this subject have already been published,[7–18] and several definitions of the effective parameters, which will be reviewed in more detail in Sec. II, have been proposed. The ultimate verification of such a definition is the comparison of the reflection coefficient of the crystal calculated rigorously with that of the effective medium. So far, such a verification has been explicitly performed only for normal[9,11,12] or near-normal[13] incidence. However, many applications, including those related to negative refraction, rely on waves incident at large angles as well as evanescent ones. The range of validity of the effective-medium approximation is, therefore, still poorly known. This paper aims to evaluate its performance in the whole range of angles of incidence, to discuss the factors responsible for its success or failure, and to provide rules enabling estimation of its validity for arbitrary two-dimensional (2D) PCs.

Consider a semi-infinite 2D PC invariant along the y axis, on whose surface, perpendicular to the z axis, an s- or p-polarized plane wave is incident [Fig. 1(a)]. Due to the crystal periodicity in the x direction, the reflected field will comprise infinitely many diffraction orders. Similarly, the transmitted field will be a combination of infinitely many crystal eigenmodes (propagative and evanescent) characterized by different wave vectors. On the contrary, if the crystal was replaced by a homogeneous material (in general, anisotropic but with one optical axis directed along y), only one transmitted plane wave would be excited. Evidently, therefore, the effective-medium approximation can be expected to give a good picture of reality only when some crystal eigenmode is excited with amplitude significantly greater than the others. Thus, the validity of the effective-medium approximation is seen to be constrained by that of the *single-mode approximation*, which consists in neglecting all crystal eigenstates except the dominant one. Note that the situation is different from the one-dimensional (1D) case, where the crystal always supports exactly two eigenmodes, only one of which is excited by an incident wave. The usefulness of the effective-medium approximation in the 1D case depends

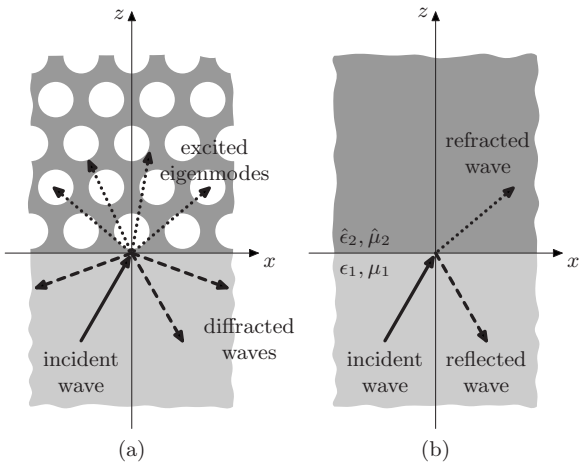

FIG. 1. Schematic diagrams of the fields generated by a polarized plane-wave incident from an isotropic homogeneous medium on the surface of (a) a photonic crystal and (b) another homogeneous medium.

mainly on the rate of variability of the effective parameters with the angle of incidence (ideally, they should not depend on it); in particular, Pierre and Gralak[14] showed that only for specific crystal truncations these parameters are continuous when the crystal eigenmode turns from propagating to evanescent.

The plan of this paper is as follows. In Sec. II, we review the definitions of the effective parameters proposed to date and give a justification of a specific one, showing it to be rigorous under the single-mode approximation. Based on that definition, in Sec. III we derive conditions for the reality and continuity of effective ϵ and μ, extending to two dimensions the results presented in Ref. 14 for 1D crystals. In Sec. IV, we proceed to the discussion of the applicability conditions of the single-mode approximation itself, formulating them in terms of the Fourier spectrum of electromagnetic fields of individual crystal eigenmodes. These results are used to show that as far as the bands responsible for negative refraction are concerned, the single-mode approximation is moderately accurate only close to normal incidence. Thus, effective ϵ and μ of the crystal corresponding to large values of the component k_x of the wave vector—in particular, to eigenstates evanescent in the z direction—are not well-defined quantities. In consequence, the behavior of systems containing homogeneous negative-index materials can change significantly if these materials are replaced with PCs, even if the equifrequency curves (EFCs) (and so the phase refractive indices) of both media are the same.

II. DEFINITION OF EFFECTIVE PARAMETERS

In the effective-medium approximation a lossless 2D PC is modeled by a lossless homogeneous, possibly anisotropic medium with one optical axis oriented along the invariant direction of the PC, hereafter taken to lie along the y axis. We shall begin with a brief analysis of the refraction of a plane-wave incident on the interface between an isotropic medium with relative permittivity ϵ_1 and permeability μ_1, occupying the $z<0$ half-space, and this anisotropic material characterized by tensorial $\hat{\epsilon}_2$ and $\hat{\mu}_2$, lying in the $z>0$ half-space [Fig. 1(b)]. The wave is taken to propagate in the xz plane. Throughout this paper we assume all electromagnetic fields to be s-polarized (electric field perpendicular to the xz plane); the analysis of the p polarization case proceeds along similar lines and will be omitted for brevity. For the sake of simplicity, we shall restrict our attention to the case when another optical axis of the anisotropic medium is perpendicular to the interface (i.e., lies along the z direction)—this corresponds to the usual case of the PC unit cell having a mirror plane perpendicular to x or z. The tensors $\hat{\epsilon}_2$ and $\hat{\mu}_2$ become then diagonal,

$$\hat{\epsilon}_2 = \begin{bmatrix} \epsilon_{2x} & 0 & 0 \\ 0 & \epsilon_{2y} & 0 \\ 0 & 0 & \epsilon_{2z} \end{bmatrix}, \quad \hat{\mu}_2 = \begin{bmatrix} \mu_{2x} & 0 & 0 \\ 0 & \mu_{2y} & 0 \\ 0 & 0 & \mu_{2z} \end{bmatrix}, \tag{1}$$

and the dispersion relation of s-polarized plane waves with wave vector $\vec{k}=k_x\hat{x}+k_z\hat{z}$ propagating in this medium takes the form

$$\frac{k_x^2}{\mu_{2z}} + \frac{k_z^2}{\mu_{2x}} = \epsilon_{2y}\frac{\omega^2}{c^2}, \tag{2}$$

where ω denotes the frequency and $c \equiv 1/\sqrt{\epsilon_0\mu_0}$ the speed of light defined in terms of the vacuum permittivity ϵ_0 and permeability μ_0. Thus, the EFCs of this material are ellipses with principal axes of length $2K_x \equiv 2\sqrt{\epsilon_{2y}\mu_{2z}}\omega/c$ and $2K_z \equiv 2\sqrt{\epsilon_{2y}\mu_{2x}}\omega/c$.

When a plane wave with wave vector $\vec{k}_1=k_x\hat{x}+k_{1z}\hat{z}$ falls on the interface between the isotropic medium 1 and the anisotropic medium 2, reflected and refracted waves are generated, with wave vectors $\vec{k}_1'=k_x\hat{x}-k_{1z}\hat{z}$ and $\vec{k}_2=k_x\hat{x}+k_{2z}\hat{z}$, respectively. By imposing the continuity conditions at $z=0$ on field components parallel to the interface, the well-known Fresnel formulas for the amplitude of the reflected and refracted waves can be derived,

$$r = \frac{\mu_{2x}/k_{2z} - \mu_1/k_{1z}}{\mu_{2x}/k_{2z} + \mu_1/k_{1z}}, \quad t = \frac{2\mu_{2x}/k_{2z}}{\mu_{2x}/k_{2z} + \mu_1/k_{1z}}. \tag{3}$$

These formulas can be written in a concise way by introducing the notion of *transverse impedance* of a material, defined as

$$\eta_{jt} = E_{jt}/H_{jt} \quad (j=1,2), \tag{4}$$

where E_{jt} (H_{jt}) is the amplitude of the transverse, i.e., parallel to the interface, component of the electric (magnetic) field of a plane wave propagating in the jth material in the given direction $\vec{k}_j$. Since in our case $E_{jt}=E_{jy}=E_{jy}^0 e^{i\vec{k}_j\cdot\vec{r}}$, $H_{1t}=-H_{1x}=(i\omega\mu_0\mu_1)^{-1}\partial E_{1y}/\partial z=(k_{1z}/\omega\mu_0\mu_1)E_{1y}$, and $H_{2t}=(k_{2z}/\omega\mu_0\mu_{2x})E_{2y}$, we obtain

$$r = \frac{\eta_{2t} - \eta_{1t}}{\eta_{2t} + \eta_{1t}} \quad t = \frac{2\eta_{2t}}{\eta_{2t} + \eta_{1t}}. \tag{5}$$

Several authors have attempted to generalize the concept of transverse impedance to nonhomogeneous media, the main obstacle being, obviously, that in such media the ratio in Eq. (4) is spatially dependent.[9,11–13,19] The most straightforward is to define η_t as the ratio of the spatial field *averages* over the surface unit cell, as proposed by Lu and Prather;[11] while this might seem an oversimplification, in the following we show that this approach is, in fact, rigorous if the single-mode approximation holds. In an attempt to preserve more information from the detailed field structure, other authors[9,12,13,19] suggested empirical definitions of the transverse impedance, expressed in terms of the average electromagnetic energy and Poynting vector of the dominant crystal eigenmode. However, no mathematical justification of these definitions has been given.

Efros and Pokrovsky[8] and later Decoopman *et al.*[10] proposed an entirely different procedure. They considered the perturbation of the incident electromagnetic field caused by a PC slab embedded in a homogeneous medium whose permittivity and permeability were varied. The values of these parameters corresponding to minimum perturbation were taken as the effective ϵ and μ of the crystal. Contrary to the single-mode approximation, such an approach is based on a rigorous solution of Maxwell equations. On the other hand, it requires significant computational effort since, for each value

of the frequency and angle of incidence, simulations need to be performed for multiple, possibly complex, values of ϵ and μ of the homogeneous medium. Therefore, it is not well suited to the analysis of the general behavior of the effective parameters, for which a—even approximate—semianalytical approach would be useful.

Finally, some authors[15–18] proposed definitions of effective parameters based on the extended Maxwell-Garnett theory, where the crystal unit cell is replaced by a coated cylinder (or sphere) embedded in a homogeneous host medium, whose parameters are determined from the condition of vanishing scattering, calculated by the Mie theory. This approach enabled them to reproduce the band structure of the PCs in question, usually composed of dispersive (e.g., polaritonic) materials, with good accuracy. Nevertheless, the effective parameters they obtained are independent of the choice of the crystal truncation plane, whereas one of the key observations of Decoopman *et al.*[10] was the strong variability of effective ϵ and μ with the position of the crystal surface. Thus, the parameters introduced in Refs. 15–18 could not be used to determine accurately the reflection coefficient of a truncated PC.

To arrive at the proper definition of the parameters in question, let us consider once again the configuration shown in Fig. 1(a), a semi-infinite 2D PC, on which a plane wave with wave vector $\vec{k}=k_x\hat{x}+k_z\hat{z}$ is incident. Since we shall focus on the case of *s* polarization, the electric field reduces to its component along the *y* axis. We assume the crystal to be oriented so that a (not necessarily primitive) rectangular unit cell (a_x,a_z) can be defined. From the Maxwell equations, we get

$$\frac{\partial E_y}{\partial x} = i\omega\mu_0\mu H_z, \tag{6a}$$

$$\frac{\partial E_y}{\partial z} = -i\omega\mu_0\mu H_x, \tag{6b}$$

$$\frac{\partial H_z}{\partial x} - \frac{\partial H_x}{\partial z} = i\omega\epsilon_0\epsilon E_y, \tag{6c}$$

where harmonic time dependence $e^{-i\omega t}$ has been assumed. These equations can be solved separately in the homogeneous and periodic region and then matched at the crystal surface $z=0$; to fulfill Maxwell boundary conditions, the continuity of the E_y and H_x components on the surface has to be assured.

The resulting structure is periodic with respect to the variable *x*, so it is possible to perform a Floquet-Bloch transform[2,20] of the Maxwell equations (6). After this transform, as it is well known from the grating theory, the solution of the Maxwell equations in the homogeneous region is given by the Rayleigh expansion,[21,22]

$$E_y^h(x,z) = e^{i(k_x x+\beta_0 z)} + \sum_{n\in\mathbb{Z}} r_n e^{i[(k_x+G_{xn})x-\beta_n z]}, \tag{7}$$

where $G_{xn}\equiv 2\pi n/a_x$ and $\beta_n\equiv[\epsilon_1\mu_1(\omega/c)^2-(k_x+G_{xn})^2]^{1/2}$ with the sign of the square root chosen so that $\mathrm{Re}\,\beta_n+\mathrm{Im}\,\beta_n\geq 0$. In the crystal, we can expand the field in terms of the PC eigenmodes with the *x* wave-vector component equal to k_x, taking into account (i) propagative modes carrying energy in the $+z$ direction and (ii) evanescent modes decaying in this direction.[2,23–28] These modes can be determined by several methods, most of which utilize some variant of the scattering-matrix algorithm;[29] in our calculations we have used the differential method.[21,30,31] The electric field of the *m*th eigenmode with wave vector $\vec{\kappa}_m\equiv k_x\hat{x}+\kappa_{mz}\hat{z}$ can be written as a 2D Fourier expansion with coefficients $(u_m^{np})_{n,p\in\mathbb{Z}}$,

$$E_{my}(x,z) = \sum_{n\in\mathbb{Z}}\sum_{p\in\mathbb{Z}} u_m^{np} e^{i[(k_x+G_{xn})x+(\kappa_{mz}+G_{zp})z]}, \tag{8}$$

where $G_{zp}\equiv 2\pi p/a_z$. Thus, the total electric field in the crystal will be

$$E_y^{\mathrm{cr}}(x,z) = \sum_{m\in\mathbb{N}} t_m E_{my}(x,z), \tag{9}$$

with "transmission coefficients" t_m denoting the amplitudes of individual modes.

The requirement of continuity of E_y and H_x at $z=0$ leads to

$$e^{ik_x x} + \sum_n r_n e^{i(k_x+G_{xn})x} = \sum_m t_m \sum_n \sum_p u_m^{np} e^{i(k_x+G_{xn})x}, \tag{10a}$$

$$\frac{i\beta_0}{\mu_1} e^{ik_x x} - \sum_n \frac{i\beta_n}{\mu_1} r_n e^{i(k_x+G_{xn})x} = \sum_m t_m \sum_n \sum_p i(\kappa_{mz}+G_{zp}) u_m^{np} e^{i(k_x+G_{xn})x}. \tag{10b}$$

Using the identity $\int_0^1 e^{2\pi i n x}dx=\delta_{n0}$, where δ_{nm} equals 1 if $n=m$ and 0 otherwise, we arrive at the following inhomogeneous system of linear equations with unknowns $(r_n)_{n\in\mathbb{Z}}$ and $(t_m)_{m\in\mathbb{N}}$:

$$\delta_{n0} + r_n = \sum_m u_m^n t_m, \tag{11a}$$

$$\frac{i\beta_n}{\mu_1}(\delta_{n0}-r_n) = \sum_m v_m^n t_m, \quad n\in\mathbb{Z} \tag{11b}$$

with the coefficients u_m^n and v_m^n defined as

$$u_m^n \equiv \sum_p u_m^{np}, \quad v_m^n \equiv \sum_p i(\kappa_{mz}+G_{zp}) u_m^{np}. \tag{12}$$

This system can be written in the matrix form,

$$\begin{bmatrix} -\hat{I} & \hat{u} \\ i\hat{\beta}/\mu_1 & \hat{v} \end{bmatrix} \begin{bmatrix} \vec{r} \\ \vec{t} \end{bmatrix} = \begin{bmatrix} \vec{a} \\ \vec{a}' \end{bmatrix}, \tag{13}$$

where $\hat{I}$ denotes the identity matrix, $\hat{u}$ and $\hat{v}$ are matrices with elements u_m^n and v_m^n (the row and column indices being denoted by superscript and subscript, respectively), $\hat{\beta}$ is the diagonal matrix of the coefficients β_n, $\vec{r}$ and $\vec{t}$ are column vectors of the coefficients r_n and t_m, and the vectors $\vec{a}$ and $\vec{a}'$, whose elements are given by

$$a_n \equiv \delta_{n0}, \quad a'_n \equiv i\beta_0\delta_{n0}/\mu_1, \tag{14}$$

represent the incident field.

If the crystal was replaced by a homogeneous medium, the only nonzero reflection coefficient would be the specular one (r_0). Using Eqs. (11a) and (11b) corresponding to $n=0$, the following relation between r_0 and the transmission coefficients of individual modes can be derived:

$$r_0 = \frac{\sum_m [u_m^0 - (\mu_1/i\beta_0)v_m^0]t_m}{\sum_m [u_m^0 + (\mu_1/i\beta_0)v_m^0]t_m}. \tag{15}$$

As we have already seen, the effective-medium approximation relies on the assumption that the transmission coefficient of a particular mode is much larger than all the others; without loss of generality, we can denote this mode with the index 1, so that our assumption reads $|t_1| \gg |t_2|, |t_3|, \cdots$. If it is fulfilled, expression (15) reduces to

$$r_0 \approx \frac{iu_1^0/v_1^0 - \mu_1/\beta_0}{iu_1^0/v_1^0 + \mu_1/\beta_0}. \tag{16}$$

Comparing this expression with Eq. (3), noting that β_0 corresponds to k_{1z}, and using the dispersion relation (2), we see that within the framework of the single-mode approximation the PC produces the same reflected wave as a homogeneous medium with

$$\mu_x = i\kappa_{1z}\frac{u_1^0}{v_1^0}, \quad \mu_z = \frac{K_x^2}{K_z^2}\mu_x, \quad \epsilon_y = \frac{1}{\mu_x}\frac{K_z^2}{\omega^2/c^2}, \tag{17}$$

with the values of K_x and K_z read from the EFC of the dominant crystal eigenmode. The transverse impedance is seen to be

$$\eta_t = i\omega\mu_0\frac{u_1^0}{v_1^0}. \tag{18}$$

This agrees with the definition of Lu and Prather (Sec. 3 in Ref. 11), since from Eqs. (6b), (8), and (12) follows that u_1^0 and $-v_1^0/(i\omega\mu_0)$ are the average electric and magnetic field, respectively, of the periodic part of the eigenmode on the PC surface.

III. INFLUENCE OF SYMMETRIES ON THE EFFECTIVE PARAMETERS

A. Symmetry requirement for reality

From Eq. (8) it follows that shifting the origin of the coordinate system by $\hat{x}\Delta x + \hat{z}\Delta z$ corresponds to the mapping

$$u_m^{np} \mapsto u_m^{np}(\Delta z) \equiv u_m^{np} e^{-i[(k_x+G_{xn})\Delta x + (\kappa_{mz}+G_{zp})\Delta z]}, \tag{19}$$

so that from Eq. (12) we obtain

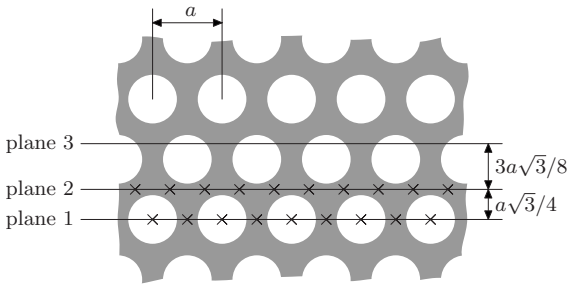

FIG. 2. The structure of the PC analyzed in the text: a hexagonal lattice of holes of radius $0.35a$ embedded in a dielectric matrix. The horizontal lines mark the position of truncation planes 1–3; inversion centers of the infinite lattice located at these planes are marked with crosses.

$$\frac{u_1^0}{v_1^0} \mapsto \frac{u_1^0(\Delta z)}{v_1^0(\Delta z)} \equiv \frac{\sum_p u_1^{0p} e^{-i(\kappa_{1z}+G_{zp})\Delta z}}{\sum_p i(\kappa_{1z}+G_{zp})u_1^{0p} e^{-i(\kappa_{1z}+G_{zp})\Delta z}}. \tag{20}$$

As expected, this ratio depends only on the position of the interface (the $z=0$ plane) but not on the exact location of the origin of the coordinate system on this plane. We are now ready to prove the first result.

Both the reflection coefficient r_0 and the effective parameters μ_x, μ_z, ϵ_y, and η_t are real provided that the following three conditions are satisfied: (i) *both the incident wave and the dominant eigenmode are propagative (β_0 and κ_{1z} are real),* (ii) *the truncation plane $z=0$ contains an inversion center of the infinite crystal, and* (iii) *the single-mode approximation is valid.*

The proof relies on the fact that the coefficients u_m^{np} of a propagating mode m can be obtained with the standard plane-wave method, and if the crystal unit cell is centrosymmetric with respect to the origin, they are elements of an eigenvector of a real symmetric matrix, hence necessarily real (in the s-polarization case additionally multiplied by a real diagonal matrix).[32] From Eq. (12), u_m^n are then real, while v_m^n are imaginary; in particular, the expression iu_1^0/v_1^0 occurring in Eqs. (16)–(18) is real. Since, by assumption, so are β_0 and κ_{1z}, the proposition follows from simple inspection of formulas (16)–(18). If the inversion center lies at $(x_0,0)$ with $x_0 \neq 0$, the above argument can be applied, too, after shifting the origin of the coordinate system by $-x_0\hat{x}$: from Eq. (20), this transformation does not change the values of r_0 or the effective parameters. On the other hand, if the interface contains no symmetry centers, a complex Hermitian eigenvalue problem must be solved in the plane-wave method, so that the eigenvector elements are not longer real, and we cannot expect iu_1^0/v_1^0 to be real either.

We remind that in the 1D case the reality of the effective parameters is guaranteed if the surface is a *mirror-symmetry plane* of the infinite crystal;[14] however, in one dimension mirror planes are, in fact, identical with inversion centers, so that *a priori* it is not obvious which of these symmetry elements prove to be crucial in two dimensions.

As an illustration of the above theorem, we shall consider the crystal shown in Fig. 2: the hexagonal lattice of air holes

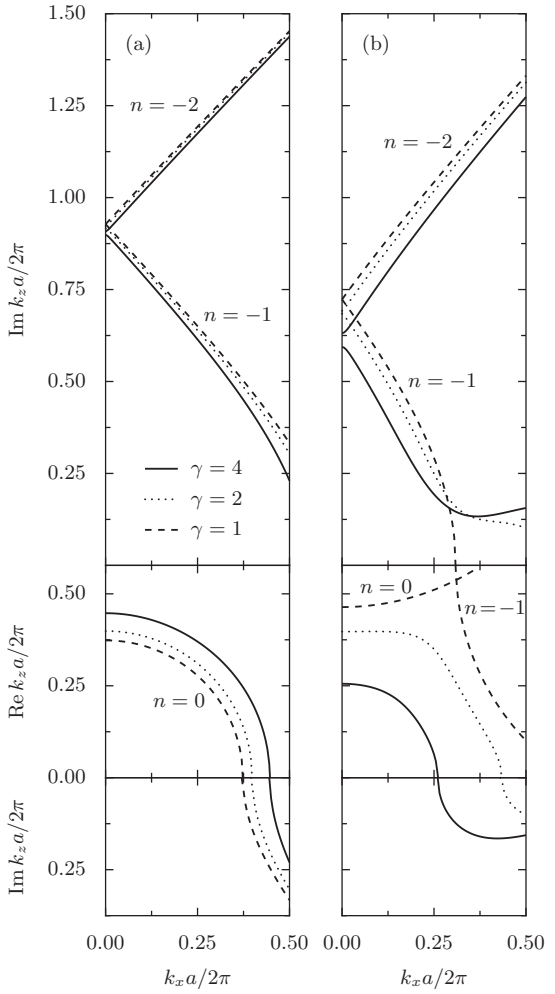

FIG. 3. The EFCs at frequency (a) $\omega=0.14\times 2\pi c/a$ and (b) $\omega=0.259\times 2\pi c/a$ of three PCs of the type shown in Fig. 2 with the same average refractive index $\langle\sqrt{\epsilon}\rangle=2.67$, but different values of the index contrast $\gamma=\sqrt{\epsilon_b}/\sqrt{\epsilon_h}$ between the background and the holes: $\epsilon_b=16$, $\epsilon_h=1$, and $\gamma=4$ (solid lines), $\epsilon_b=11.76$, $\epsilon_h=2.94$, and $\gamma=2$ (dotted lines), and $\epsilon_b=\epsilon_h=7.11$ and $\gamma=1$ (dashed lines). The middle part of the graphs shows the EFCs of the real bands (Re $k_z\neq 0$, Im $k_z=0$), the bottom one, of the imaginary bands of the first kind according to the classification of Ref. 33 (Re $k_z=0$, Im $k_z\neq 0$), and the top one, of the imaginary bands of the second kind (Re $k_z=2\pi/a\sqrt{3}$, Im $k_z\neq 0$, i.e., lying on the edge of the first Brillouin zone). Only the three bands with lowest values of Im k_z are shown in each case. The bands of the empty lattice ($\gamma=1$) are labeled with the index n of the harmonic G_{xn} to which they correspond. For each mode with wave vector $\vec{k}$ visible in the graph, the crystal supports three additional modes with wave vectors $\vec{k}^*$, $-\vec{k}$, and $-\vec{k}^*$, where the asterisk denotes complex conjugation (Ref. 33).

of radius $0.35a$, a being the lattice constant, embedded in a dielectric matrix with $\epsilon=16$. At the frequency $\omega=0.14\times 2\pi c/a$, the EFC of the single s-polarized propagating crystal eigenmode is circular [Fig. 3(a), middle diagram, solid line]. In Figs. 4(a), 4(c), and 4(e) the specular reflection coefficient of this crystal at the cited frequency value is plotted against the x component of the wave vector of the incident plane wave for three different positions of the interface between the crystal and the homogeneous medium, taken to be

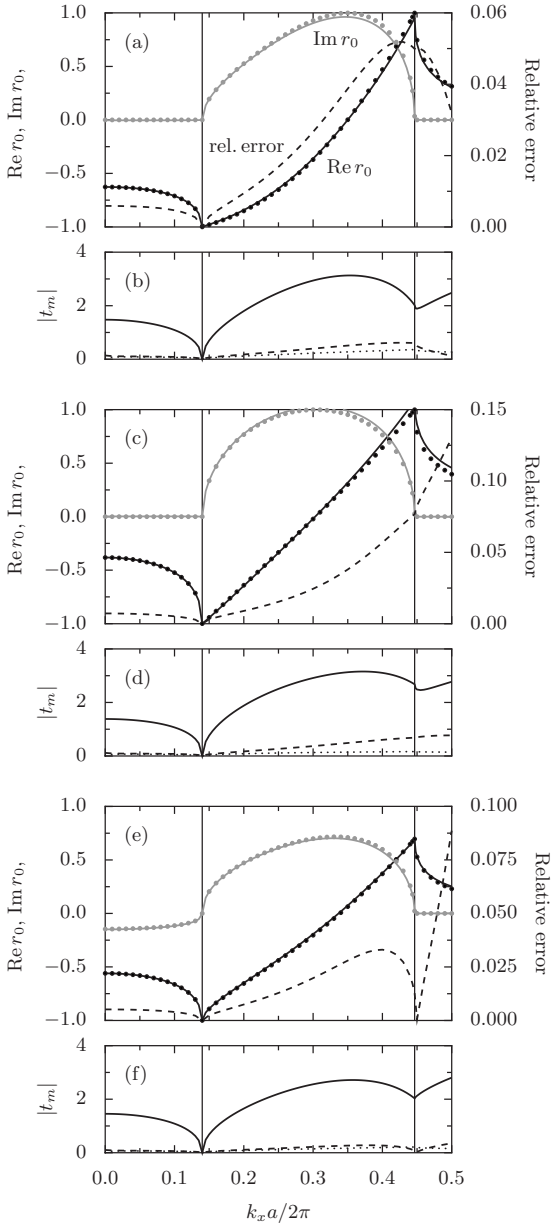

FIG. 4. (a) The k_x dependence of the specular reflection coefficient r_0 of the crystal from Fig. 2 truncated along plane 1 at $\omega=0.14\times 2\pi c/a$. Solid lines: results of rigorous calculations; circles: results of calculations made in the single-mode approximation; and dashed line: relative error of the single-mode approximation, $|r_{\text{singlemode}}-r_{\text{rigorous}}|/|r_{\text{rigorous}}|$. The vertical lines at $k_x=0.14\times 2\pi/a$ and $0.4465\times 2\pi/a$ mark where the incident wave and the single propagating crystal eigenmode, respectively, turn from propagating to evanescent. (b) Amplitudes of the three most slowly decaying crystal eigenmodes excited in the above conditions (solid, dashed, and dotted lines in order of increasing Im k_z). [(c) and (d)] The same for plane 2. [(e) and (f)] The same for plane 3.

vacuum ($\varepsilon_1=\mu_1=1$). Evidently, for surfaces containing inversion centers [Figs. 4(a) and 4(c)] Im r_0 is very small in the whole range $k_x<0.14\times 2\pi/a$, where the incident wave is propagative. On the contrary, when the termination is chosen in an arbitrary way [Fig. 4(e)], r_0 has an appreciable imaginary part. In all three graphs, the relative error of the single-

mode approximation, defined as $|r_{\text{singlemode}} - r_{\text{rigorous}}|/|r_{\text{rigorous}}|$, is plotted with a dashed line. It is clear that at the chosen frequency (corresponding to the middle of the first crystal band) the single-mode approximation is very accurate for k_x corresponding to propagating incoming waves ($k_x < \omega/c$); for larger k_x, accuracy degrades slightly, but the relative error seldom exceeds 10%.

B. Symmetry requirement for continuity

We proceed to the investigation of the behavior of the effective permittivity and permeability near the value of k_x at which the dominant eigenmode transforms from propagating to evanescent. At this point, κ_{1z} is zero; according to Eq. (17), this implies $\mu_x = \mu_z = 0$ and $|\varepsilon_y| \to \infty$ unless v_1^0 *is zero at the same time*. The italicized statement is thus a necessary condition for the continuity and boundedness of ϵ_y. We shall now show that this condition can be related to the symmetry of the eigenmode fields in the following way: *The effective parameters* μ_x, μ_z, *and* ϵ_y *are continuous only if the following conditions are satisfied:* (i) *the crystal has mirror planes parallel to the surface,* (ii) *the electric field of the dominant mode with wave vector parallel to these mirror planes is symmetric with respect to them, and* (iii) *the crystal is truncated along either* (a) *a mirror plane or* (b) *any plane containing inversion centers and parallel to the mirror planes, provided the latter contain inversion centers, too.*

To begin with, we note that according to the group theory,[34,35] the crystal eigenmodes with a given wave vector $\vec{k}$ can be classified in terms of the irreducible representations of the largest common subgroup of the photonic lattice group and the group of $\vec{k}$, i.e., the group of symmetry operations leaving the wave-vector invariant. For $\vec{k}$ parallel to x the latter group comprises only the identity I and the reflection with respect to the x axis, σ_x. It follows that if the crystal itself has a mirror plane parallel to x, the electric field of the eigenmodes with $\vec{k} = k_x \hat{x}$ is either symmetric or antisymmetric with respect to reflection about it. Let us assume this plane to lie at $z=0$. From Eqs. (12) and (20) it follows that the "shifted" coefficient $v_1^0(z_0)$ will be

$$v_1^0(z_0) = \frac{2\pi i}{a_z} \sum_p p u_1^{0p} e^{-2\pi i p z_0/a_z}. \tag{21}$$

If the electric field is *symmetric* with respect to the plane $z=0$, we have $u_1^{np} = u_1^{n,-p}$ for all $n, p \in \mathbb{Z}$, hence

$$v_1^0(z_0) = \frac{4\pi}{a_z} \sum_{p>0} p u_1^{0p} \sin\frac{2\pi p z_0}{a_z}. \tag{22}$$

Without further constraints on u_1^{0p}, the coefficient $v_1^0(z_0)$ will be null only if $2\pi z_0/a_z$ is an integral multiple of π, so that all the sine factors vanish. With z_0 restricted to the first unit cell ($0 \le z_0 < a_z$), this is equivalent to $z_0 = 0$ or $z_0 = a_z/2$. Thus, the truncation must coincide with one of the mirror planes (obviously, $z = a_z/2$ is a mirror plane if $z=0$ is one).

Assume now that the crystal has inversion centers outside the mirror planes. It is easy to see that they must lie halfway between successive planes, i.e., at $z = a_z/4$ and $z = 3a_z/4$. As shown in Sec. III A, the coefficients $u_1^{np}(a_z/4)$ and $u_1^{np}(3a_z/4)$ must then be real; from Eq. (19), $u_1^{np}(a_z/4) \equiv u_1^{np} e^{-2\pi i p/4} = u_1^{np}(-i)^p$, so the reality condition reads

$$u_1^{np}(-i)^p = (u_1^{np})^* i^p. \tag{23}$$

It follows that

$$u_1^{np} \text{ is } \left\{ \begin{matrix} \text{real} \\ \text{imaginary} \end{matrix} \right\} \text{ for all } \left\{ \begin{matrix} \text{even} \\ \text{odd} \end{matrix} \right\} p. \tag{24}$$

Alone, this condition does not ensure vanishing of v_1^0 at any new truncation planes. However, if the mirror plane $z=0$ also contains inversion centers, then all the coefficients u_1^{np} must be real. Combined with (24), this means that u_1^{np} vanish for all odd p, and expression (22) for $v_1^0(z_0)$ becomes

$$v_1^0(z_0) = \frac{4\pi}{a_z} \sum_{p>0} 2p u_1^{0,2p} \sin\frac{4\pi p z_0}{a_z}. \tag{25}$$

It will be null provided that $z_0 = n a_z/4$, with $n \in \mathbb{Z}$, i.e., on all planes containing inversion centers.

Let us now proceed to the case of electric-field *antisymmetric* to the mirror planes. We have then $u_1^{np} = -u_1^{n,-p}$, and the sines in Eq. (22) are replaced by cosines. In order that $v_1^0(z_0)$ is null, to each $p \in \mathbb{N}$ must correspond a $q \in \mathbb{Z}$ such that $2\pi p z_0/a_z = (q + \frac{1}{2})\pi$. It is easy to see that this condition cannot be fulfilled for any value of z_0. If the structure has additional inversion centers, so that u_1^{np} vanish for all odd p, the condition becomes $4\pi p z_0/a_z = (q + \frac{1}{2})\pi$, which has no solutions, either.

The above considerations show that if the PC has no mirror planes parallel to the surface, there will be no interplay between coefficients u_1^{np} and $u_1^{n,-p}$, which is necessary so that all the terms of the series in Eq. (21) vanish. It should be emphasized that presence of different symmetry elements, such as mirror planes *perpendicular* to the surface, will not change matters, since these operations are not in the group of the wave vector $\vec{k} = k_x \hat{x}$.

As an illustration of the above theorem, consider again the structure from Fig. 2. In Figs. 5 and 6 the k_x dependence of the effective μ_x and ϵ_y for different frequencies and termination planes is shown. In the first band (Fig. 5), the electric field has the required symmetry, so that for truncation planes 1 and 2 $\epsilon_y(k_x)$ is continuous, whereas it is divergent for the arbitrarily chosen plane 3. On the contrary, the electric field of a mode belonging to the second band is antisymmetric with respect to the mirror planes (Fig. 6), and so ϵ_y is divergent no matter what truncation plane is chosen.

C. Remarks

In the context of metamaterials containing resonant components, such as split rings, it has been observed that inside band gaps, the effective permittivity and permeability of these structures (defined at normal incidence) have large imaginary parts of opposite sign, regardless of the truncation plane location.[36–39] This is not in contradiction with our theory, since one of the assumptions of the condition for reality of ϵ and μ formulated in Sec. III A is the propagative nature of the fundamental crystal eigenstate (real κ_{1z}). Of course, inside band gaps all modes are evanescent, and so the above condition is not applicable.

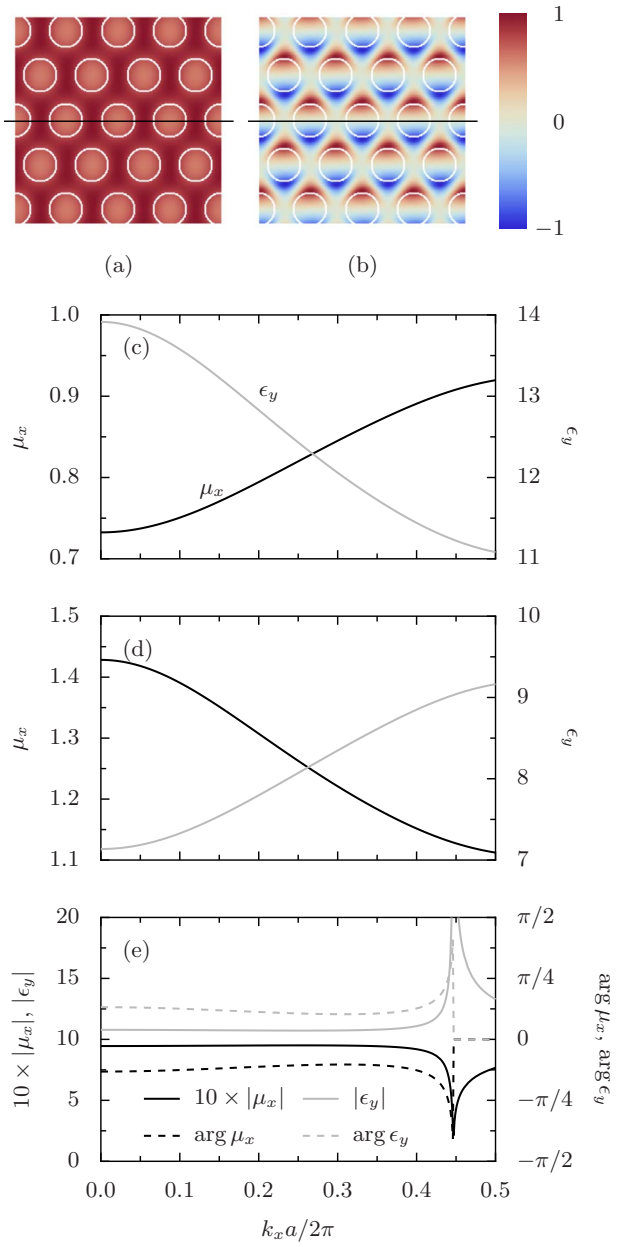

FIG. 5. (Color online) (a) Electric field E_y and (b) magnetic field H_x of the single propagating mode with $\vec{\kappa} \| \hat{x}$ of the crystal shown in Fig. 2 at $\omega = 0.14 \times 2\pi c/a$. A sample mirror plane of the lattice parallel to the crystal surface is marked with a horizontal line. [(c)–(e)] Effective μ_x (dark lines) and ϵ_y (light lines) of this crystal at the same frequency for truncation planes 1–3.

On the other hand, our results show that, in general, the effective parameters of a lossless PC can attain complex values even outside band gaps, if the truncation plane does not exhibit certain symmetries. In this case, the product $\epsilon\mu$ is real (due to the absence of losses), and either ε or μ has negative imaginary part. This is visible, for example, in Fig. 5(e) showing the k_x dependence of the effective parameters for the low-symmetric truncation plane 3: it is clear that $\arg \mu_x \in [-\frac{\pi}{2}, 0]$, so that $\mathrm{Im}\, \mu_x < 0$. Only at specific truncation planes effective ϵ and μ are real. (It must be noted, though, that precisely these special truncation planes have usually been chosen in previous calculations of the effective parameters of PCs and metamaterials.)

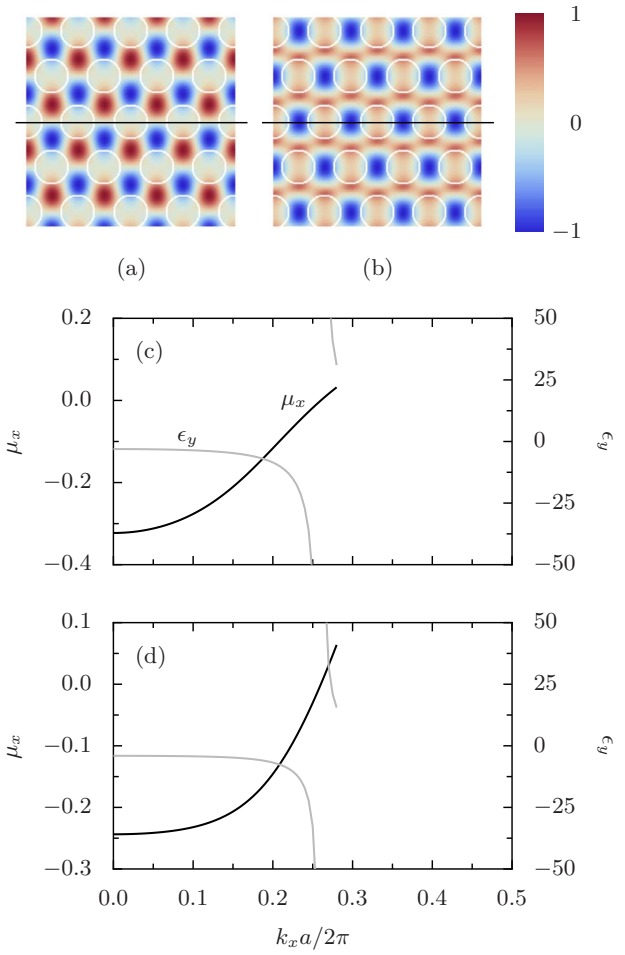

FIG. 6. (Color online) Same as in Fig. 5 at frequency $\omega = 0.259 \times 2\pi c/a$ and for truncation planes (c) 1 and (d) 2. The plot domains have been restricted to the k_x range in which the relative error of the single-mode approximation is less than approximately 25% (cf. Fig. 7).

To conclude this section, we stress that the symmetry requirements we have derived are *rigorous* in the framework of the single-mode approximation. Excitation of secondary crystal eigenmodes will perturb the true reflection coefficient, e.g., introducing a small imaginary part even though the truncation plane contains inversion centers. Nevertheless, if the perturbation is not too strong, the presented conditions are still useful, for instance, in searching for the crystal truncation with $\mathrm{Im}\, r_0$ as small as possible.

IV. VALIDITY OF THE SINGLE-MODE APPROXIMATION

We have seen that at a frequency value belonging to the first band of the crystal shown in Fig. 2, the single-mode approximation works well, and so the effective-medium model is well founded (cf. Fig. 4). In the second band, however, this approximation becomes much less accurate. In Figs. 7(a) and 7(c), the rigorous value of the specular reflection coefficient of the crystal at the frequency $\omega = 0.259$

$\times 2\pi c/a$ is juxtaposed with that calculated from Eq. (16); the relative error grows with k_x and is usually greater than 20% (plane 1) and 10% (plane 2). In the evanescent region, the single-mode approximation is clearly irrelevant. The graphs of the amplitudes of the three most slowly decaying crystal eigenmodes [Figs. 7(b) and 7(d)] show that the influence of the second mode is non-negligible in the whole range of k_x, and for the first truncation plane, even the third mode plays a significant part. Close inspection reveals that the ratios $|t_2/t_1|$ and $|t_3/t_1|$ tend to grow with the incidence angle; thus, the effective-medium model is a better approximation at near-normal than at grazing incidence (except for the immediate neighborhood of $k_x=\omega/c$, where r_0 becomes exactly -1).

It is natural to ask about the reason underlying the high amplitude of the secondary modes; an answer to this question would enable us to estimate the range of applicability of the single-mode approximation. In the following, we offer a qualitative argument relating the ratios $|t_m/t_1|$ to the Fourier spectrum of the individual mode fields on the crystal surface.

Let us begin by writing system (13) in a partitioned form, emphasizing the rows corresponding to the nonzero elements of the vectors representing the incident field, a_0 and a_0', as well as the columns corresponding to the unknowns r_0 and t_k,

$$\begin{bmatrix} -\hat{I} & \vec{0} & \hat{0} & \hat{u}_{<k}^{<0} & \vec{u}_k^{<0} & \hat{u}_{>k}^{<0} \\ \bar{0} & -1 & \bar{0} & \bar{u}_{<k}^{0} & u_k^0 & \bar{u}_{>k}^{0} \\ \hat{0} & \vec{0} & -\hat{I} & \hat{u}_{<k}^{>0} & \vec{u}_k^{>0} & \hat{u}_{>k}^{>0} \\ i\hat{\beta}_{<0}/\mu_1 & \vec{0} & \hat{0} & \hat{v}_{<k}^{<0} & \vec{v}_k^{<0} & \hat{v}_{>k}^{<0} \\ \bar{0} & i\beta_0/\mu_1 & \bar{0} & \bar{v}_{<k}^{0} & v_k^0 & \bar{v}_{>k}^{0} \\ \hat{0} & \vec{0} & i\hat{\beta}_{>0}/\mu_1 & \hat{v}_{<k}^{>0} & \vec{v}_k^{>0} & \hat{v}_{>k}^{>0} \end{bmatrix} \begin{bmatrix} \vec{r}_{<0} \\ r_0 \\ \vec{r}_{>0} \\ \vec{t}_{<k} \\ t_k \\ \vec{t}_{>k} \end{bmatrix} = \begin{bmatrix} \vec{0} \\ 1 \\ \vec{0} \\ \vec{0} \\ i\beta_0/\mu_1 \\ \vec{0} \end{bmatrix}. \tag{26}$$

In the notation used, the symbols embellished with arrows, bars, and hats are column vectors, row vectors, and matrices, respectively, while those without any embellishment are scalars. The meaning of the indices should be clear; for example, $\hat{u}_{<k}^{<0}$ stands for the submatrix of the $\hat{u}$ matrix corresponding to rows with negative indices and columns with indices less than k. From the Cramer's formula, we have $t_l/t_k=D_l/D_k$, where D_j stands for the determinant of the matrix created by replacing the jth column in the matrix of the system from Eq. (26) by the right-hand side of the system. After some algebra, where elementary properties of determinants are utilized, we arrive at

$$\frac{t_l}{t_k}=(-1)^{l-k}\frac{\begin{vmatrix} -\hat{I} & \hat{0} & \hat{u}_{<l}^{<0} & \hat{u}_{>l}^{<0} \\ \hat{0} & -\hat{I} & \hat{u}_{<l}^{>0} & \hat{u}_{>l}^{>0} \\ i\hat{\beta}_{<0}/\mu_1 & \hat{0} & \hat{v}_{<l}^{<0} & \hat{v}_{>l}^{<0} \\ \hat{0} & i\hat{\beta}_{>0}/\mu_1 & \hat{v}_{<l}^{>0} & \hat{v}_{>l}^{>0} \end{vmatrix}}{\begin{vmatrix} -\hat{I} & \hat{0} & \hat{u}_{<k}^{<0} & \hat{u}_{>k}^{<0} \\ \hat{0} & -\hat{I} & \hat{u}_{<k}^{>0} & \hat{u}_{>k}^{>0} \\ i\hat{\beta}_{<0}/\mu_1 & \hat{0} & \hat{v}_{<k}^{<0} & \hat{v}_{>k}^{<0} \\ \hat{0} & i\hat{\beta}_{>0}/\mu_1 & \hat{v}_{<k}^{>0} & \hat{v}_{>k}^{>0} \end{vmatrix}}. \tag{27}$$

By means of the Laplace expansion of the determinants in the numerator and denominator along the columns containing $\vec{u}_k$ and $\vec{u}_l$, respectively, the ratio t_l/t_k can be written as the ratio of two sums of terms proportional, respectively, to the components of the Fourier expansion of the electric and magnetic fields at the crystal surface of the kth and lth eigenmode,

$$\frac{t_l}{t_k}=\frac{\sum_{n\neq 0}(a_n u_k^n+b_n v_k^n)}{\sum_{n\neq 0}(a_n u_l^n+b_n v_l^n)}, \tag{28}$$

where a_n and b_n denote the appropriate coefficients resulting from the Laplace expansion. It is crucial to observe that these sums do not contain the *zeroth* Fourier component of either field.

The PC bands can be treated as mixtures of the eigenstates of the empty lattice with "average" ϵ and μ; for a fixed k_x, these eigenstates are the plane waves $E_{yn}(x,z)=\exp[i(k_x+G_{xn})x+ik_{zn}z]$, where $k_{zn}=\sqrt{\epsilon\mu(\omega/c)^2-(k_x+G_{xn})^2}$. When the index contrast of the photonic lattice is low enough, in some regions of the (ω,k_x) space each of the PC eigenstates comprises a single dominant plane wave, the perturbative components having low amplitude. This means that each of the sets of coefficients $(u_m^n)_{n\in\mathbb{Z}}$ corresponding to different modes m contains a single dominant component. From Eq. (28) it follows that, in general, the mode whose dominant component is the zeroth one $(n=0)$ is then excited the most strongly. Indeed, labeling this mode with index $m=1$, we see that in expression (28) for the ratio t_1/t_k $(k\neq 1)$ the sum in the denominator does not contain terms proportional to u_1^0 and v_1^0, which, by assumption, are the largest ones. On the contrary, the sum in the numerator contains two terms proportional to the dominant components of the kth mode, say, $u_k^{n_k}$ and $v_k^{n_k}$, since n_k is necessarily different from zero. Thus, we see that the fraction t_1/t_k is a ratio of a "large" and a "small" quantity—and so $|t_1|\gg|t_k|$ for all $k\neq 1$, that is, the defining assumption of the single-mode approximation is fulfilled.

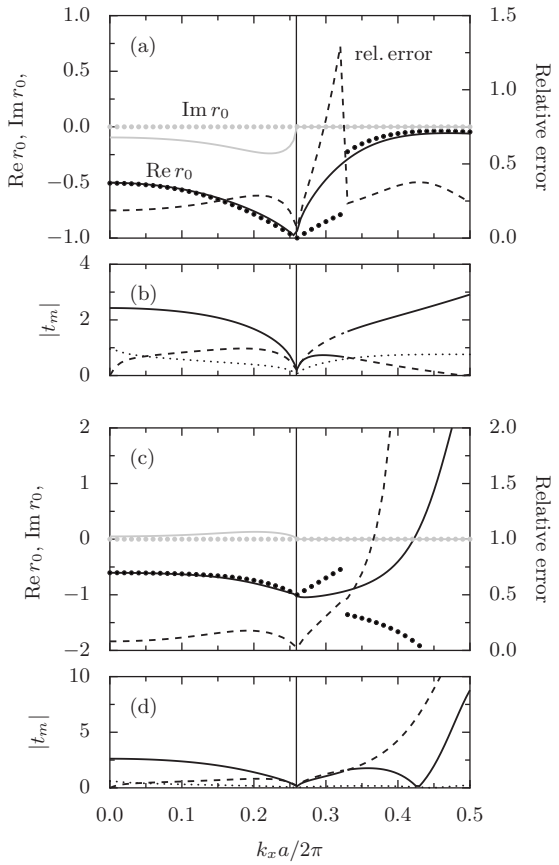

FIG. 7. Same as Fig. 4, at frequency $\omega=0.259\times 2\pi c/a$ and for truncation planes [(a) and (b)] 1 and [(c) and (d)] 2. Discontinuities in the plots of r_0 calculated in the single-mode approximation appear at $k_x=0.33\times 2\pi/a$ because at this value of k_x the two most slowly decaying crystal eigenstates "swap places," and the calculations of r_0 are always done for the mode with the smallest value of Im k_y.

Conversely, if there is strong coupling between the zeroth harmonic and plane waves corresponding to different values of n, so that no mode with highly dominant zeroth component exists, the denominator in Eq. (28) for $l=1$ is no longer a small quantity, and multiple eigenmodes can be excited with comparable amplitude.

We conclude that *the single-mode approximation should work best at those values of* ω *and* k_x *for which the mode originating from the* $n=0$ *harmonic [the plane wave* $\exp(ik_x x+ik_{z0}z)$*] does not contain significant contributions of other plane waves.* In practice, this usually means that when we consider the transition from the empty lattice to the final PC, the fragment of the PC EFC around a given value of k_x should form mainly from the circle corresponding to the $n=0$ harmonic of the empty lattice. For example, as can be seen in Fig. 3(a), the EFC of the single propagating mode of the crystal in question (solid line, middle diagram) is very similar to the original EFC of the $n=0$ harmonic of the empty lattice (dashed line). In addition, the imaginary bands corresponding to $n=-1$ and $n=-2$ are very weakly perturbed (top diagram). We infer that the individual plane waves couple weakly, so that the zeroth harmonic of the field of the propagating crystal eigenmode should be dominant, and the eigenmode itself should be strongly excited. These claims are corroborated by Figs. 8(a) and 8(b), where the amplitudes of several harmonics u_1^n and v_1^n of this mode at the truncation plane 1 are shown for two values of k_x, and Fig. 4(b), where the amplitudes $|t_m|$ of individual eigenstates are juxtaposed.

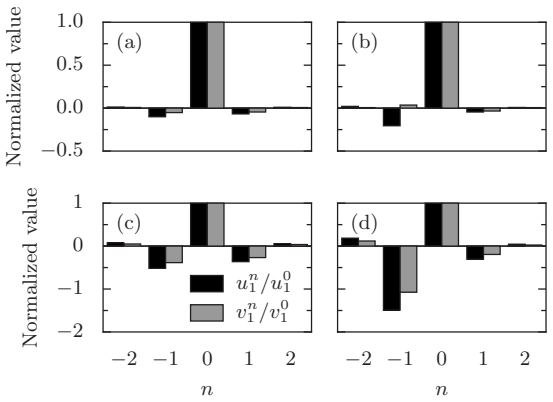

FIG. 8. Values of the harmonics $(u_1^n)^2_{n=-2}$ and $(v_1^n)^2_{n=-2}$ of the propagating eigenmode of the crystal from Fig. 2 on the truncation plane 1 and at (a) $\omega=0.14\times 2\pi c/a$, $k_x=0.10\times 2\pi/a$, (b) $\omega=0.14\times 2\pi c/a$, $k_x=0.40\times 2\pi/a$, (c) $\omega=0.259\times 2\pi c/a$, $k_x=0.05\times 2\pi/a$, and (d) $\omega=0.259\times 2\pi c/a$, $k_x=0.20\times 2\pi/a$.

Now let us turn our attention to Fig. 3(b), where the evolution of the EFCs at the frequency $\omega=0.259\times 2\pi a/c$ is shown; this frequency lies in the second band, which exhibits negative group velocity. We can see that in this case the plotted quarter of the circular EFC of the single propagating crystal eigenstate is formed by merging of the $n=0$ and $n=-1$ harmonics of the empty lattice. Their strong coupling is further indicated by the substantial alteration of the shape of the imaginary bands. We can expect the contribution of the zeroth harmonic to be the strongest at small values of k_x and so the accuracy of the single-mode approximation to be highest near normal incidence and deteriorate with increasing k_x. This is again confirmed by Figs. 8(c), 8(d), and 7(b).

To help establish a broader picture of the single-mode approximation's performance, in Fig. 9(b) the relative error of the reflection coefficient r_0 calculated in this approximation is plotted for a mesh of 101×100 points of the (k_x,ω) space. In turn, Figs. 9(c) and 9(d) present the amplitude variations of the zeroth harmonic of the electric and magnetic fields, respectively, of the most slowly decaying crystal mode (on the truncation plane 1). It can be seen that, while there is no one-to-one correspondence, the areas of significant error generally match those in which the $n=0$ component of either the electric or magnetic field, or both, of the least-evanescent eigenmode has small amplitude. (In fact, the dependence of the approximation's accuracy on the Fourier spectrum of the magnetic field seems more pronounced than that on the electric field.)

Finally, it should be noted that the EFC from Fig. 3(b) is, in fact, typical for negative-refraction bands. Indeed, the EFCs of the empty lattice are circular, with group velocity directed outward, and the negative bands arise from convex figures formed by arcs of three, four, or six such intersecting circles, necessarily including those corresponding to harmonics with nonzero G_{xn} (see Fig. 10). Thus, the resulting bands

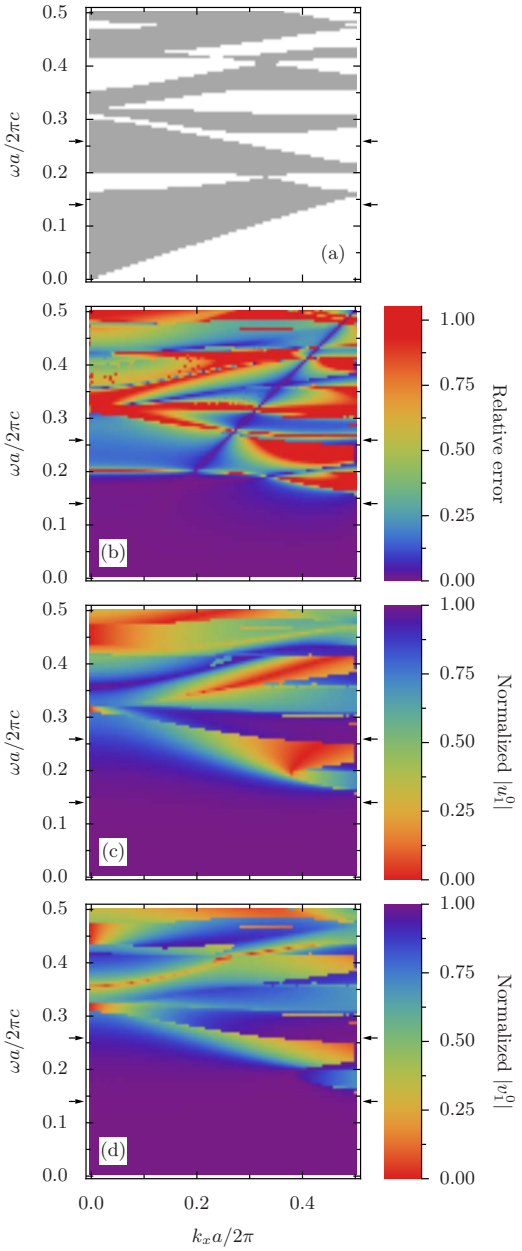

FIG. 9. (Color online) (a) The band structure of the PC shown in Fig. 2: gray and white areas denote photonic bands and gaps, respectively. The arrows mark the frequency values $\omega=0.14\times 2\pi c/a$ and $0.259\times 2\pi c/a$. (b) The dependence of the relative error of the single-mode approximation of this crystal's reflection coefficient on k_x and ω for the truncation plane 1. (c) The corresponding dependence of $|u_1^0|/[\sum_n (u_1^n)^2]^{1/2}$. (d) Same for $|v_1^0|/[\sum_n (v_1^n)^2]^{1/2}$.

do not fulfill the validity condition of the single-mode approximation or do it only in the restricted range of k_x close to zero. Consequently, attribution of effective permittivity and permeability to negative-refraction bands makes sense at most for near-normal incidence, while in the evanescent regime the effective-medium description is definitely inappropriate.

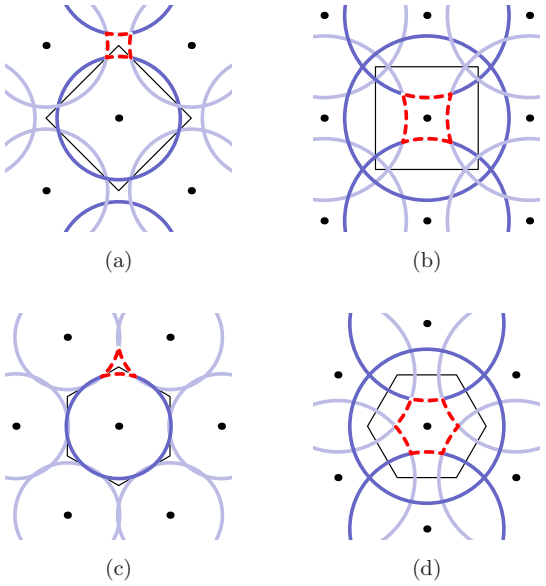

FIG. 10. (Color online) Typical configurations of empty-lattice EFCs leading to formation of negative-refraction bands (red dashed line) after introducing sufficient lattice modulation. In each case, the direction of normal incidence is from the bottom; circles corresponding to harmonics with $G_{xn}=0$ are drawn in darker blue. Thin lines mark the boundaries of the first Brillouin zone of each lattice, and black dots denote reciprocal-lattice points. Top row: square lattice, bands encircling (a) the M point of the first Brillouin zone and (b) the Γ point; bottom row: hexagonal lattice, bands encircling (c) the J point and (d) the Γ point.

V. CONCLUSIONS

In this paper, we have analyzed in detail the effective-medium description of 2D PCs. Its validity has been shown to be restricted by the accuracy of the single-mode approximation, and a definition of the effective parameters such as permittivity, permeability, and transverse impedance rigorous under this approximation has been given. In the framework of the single-mode approximation, we have studied the dependence of the reflection coefficient r of the crystal on the position of the truncation plane, deriving the conditions assuring r, and consequently the effective parameters, to be real valued. Continuity and boundedness of the latter have been shown to depend on the symmetry of the dominant crystal eigenmode. Subsequently, the conditions of validity of the single-mode approximation have been studied. We have established a link between the relative excitation amplitudes of individual crystal eigenmodes and the Fourier spectrum of the electric and magnetic fields of these modes on the crystal truncation plane. This link has been employed to formulate a qualitative criterion enabling estimation of the accuracy of the single-mode approximation based on the comparison between the equifrequency diagrams of the PC and of the homogeneous medium with refractive index equal to the average refractive index of the former. Finally, we discussed the special case of negative-refraction bands; we

concluded that the effective-medium description of these bands is, quite generally, inaccurate, since their Fourier-space structure entails simultaneous excitation of other bands by plane waves incident at most angles, and so attributing a definite effective permittivity and permeability to these bands is not physically meaningful.

ACKNOWLEDGMENTS

Thanks are due to Stefan Enoch for useful discussions. This work was partly supported by the project FANI (Grant No. ANR-07-NANO-038-03) of the program PNANO funded by the Agence Nationale de la Recherche.

*wojciech.smigaj@fresnel.fr
†boris.gralak@fresnel.fr

[1] S. Enoch, G. Tayeb, and B. Gralak, IEEE Trans. Antennas Propag. **51**, 2659 (2003).
[2] B. Gralak, S. Enoch, and G. Tayeb, in *Metamaterials: Physics and Engineering Explorations*, edited by N. Engheta and R. W. Ziolkowski (Wiley, New York, 2006), Chap. 10, pp. 261–283.
[3] H. Kosaka, T. Kawashima, A. Tomita, M. Notomi, T. Tamamura, T. Sato, and S. Kawakami, Appl. Phys. Lett. **74**, 1212 (1999).
[4] H. Kosaka, T. Kawashima, A. Tomita, M. Notomi, T. Tamamura, T. Sato, and S. Kawakami, Phys. Rev. B **58**, R10096 (1998).
[5] B. Gralak, S. Enoch, and G. Tayeb, J. Opt. Soc. Am. A **17**, 1012 (2000).
[6] J. B. Pendry, Phys. Rev. Lett. **85**, 3966 (2000).
[7] J. Ushida, M. Tokushima, M. Shirane, A. Gomyo, and H. Yamada, Phys. Rev. B **68**, 155115 (2003).
[8] A. Efros and A. Pokrovsky, Solid State Commun. **129**, 643 (2004).
[9] R. Biswas, Z. Y. Li, and K. M. Ho, Appl. Phys. Lett. **84**, 1254 (2004).
[10] T. Decoopman, G. Tayeb, S. Enoch, D. Maystre, and B. Gralak, Phys. Rev. Lett. **97**, 073905 (2006).
[11] Z. Lu and D. W. Prather, Opt. Express **15**, 8340 (2007).
[12] B. Momeni, A. Asghar Eftekhar, and A. Adibi, Opt. Lett. **32**, 778 (2007).
[13] B. Momeni, M. Badieirostami, and A. Adibi, J. Opt. Soc. Am. B **24**, 2957 (2007).
[14] R. Pierre and B. Gralak, J. Mod. Opt. **55**, 1759 (2008).
[15] Y. Wu, J. Li, Z.-Q. Zhang, and C. T. Chan, Phys. Rev. B **74**, 085111 (2006).
[16] V. Yannopapas and A. Moroz, J. Phys.: Condens. Matter **17**, 3717 (2005).
[17] V. Yannopapas and N. V. Vitanov, Phys. Rev. B **74**, 193304 (2006).
[18] V. Yannopapas, Phys. Rev. B **75**, 035112 (2007).
[19] S. Boscolo, C. Conti, M. Midrio, and C. G. Someda, J. Lightwave Technol. **20**, 304 (2002).
[20] P. Kuchment, *Floquet Theory for Partial Differential Equations* (Birkhäuser, Basel, 1993).
[21] M. Nevière and E. Popov, *Light Propagation in Periodic Media: Differential Theory and Design* (Dekker, New York, 2002).
[22] R. Petit, in *Electromagnetic Theory of Gratings*, edited by R. Petit (Springer, Berlin, 1980), Chap. 1, pp. 1–52.
[23] E. Istrate, A. A. Green, and E. H. Sargent, Phys. Rev. B **71**, 195122 (2005).
[24] Z.-Y. Li and K.-M. Ho, Phys. Rev. B **68**, 155101 (2003).
[25] L. C. Botten, T. P. White, A. A. Asatryan, T. N. Langtry, C. Martijn de Sterke, and R. C. McPhedran, Phys. Rev. E **70**, 056606 (2004).
[26] N. Stefanou, V. Karathanos, and A. Modinos, J. Phys.: Condens. Matter **4**, 7389 (1992).
[27] N. Stefanou, V. Yannopapas, and A. Modinos, Comput. Phys. Commun. **113**, 49 (1998).
[28] N. Stefanou, V. Yannopapas, and A. Modinos, Comput. Phys. Commun. **132**, 189 (2000).
[29] L. Li, J. Opt. Soc. Am. A **13**, 1024 (1996).
[30] P. Vincent, in *Electromagnetic Theory of Gratings*, edited by R. Petit (Springer, Berlin, 1980), Chap. 4, pp. 101–122.
[31] E. Popov and B. Bozhkov, Appl. Opt. **39**, 4926 (2000).
[32] M. Plihal and A. A. Maradudin, Phys. Rev. B **44**, 8565 (1991).
[33] Y.-C. Chang, Phys. Rev. B **25**, 605 (1982).
[34] K. Sakoda, *Optical Properties of Photonic Crystals* (Springer, Berlin, 2001), Chap. 3, pp. 43–80.
[35] M. Tinkham, *Group Theory and Quantum Mechanics* (McGraw-Hill, New York, 1964), Chap. 8, pp. 267–316.
[36] T. Koschny, P. Markoš, D. R. Smith, and C. M. Soukoulis, Phys. Rev. E **68**, 065602(R) (2003).
[37] D. Seetharamdoo, R. Sauleau, K. Mahdjoubi, and A.-C. Tarot, J. Appl. Phys. **98**, 063505 (2005).
[38] T. Koschny, P. Markoš, E. N. Economou, D. R. Smith, D. C. Vier, and C. M. Soukoulis, Phys. Rev. B **71**, 245105 (2005).
[39] R. Liu, T. J. Cui, D. Huang, B. Zhao, and D. R. Smith, Phys. Rev. E **76**, 026606 (2007).